

Kirigami interactive triboelectric mechanologic[☆]

Lan Luo ^{a,b,1}, Jing Han ^{b,c,1}, Yao Xiong ^{b,c}, Ziwei Huo ^{b,c}, Xiaozhen Dan ^{a,b}, Jinran Yu ^{b,c}, Jiahong Yang ^{a,b}, Linlin Li ^{a,b,c}, Jia Sun ^d, Xiaoyin Xie ^{e,*}, Zhong Lin Wang ^{b,c,f,**}, Qijun Sun ^{a,b,c,***}

^a Center on Nanoenergy Research, School of Chemistry and Chemical Engineering, Guangxi University, Nanning 530004, China

^b Beijing Institute of Nanoenergy and Nanosystems, Chinese Academy of Sciences, Beijing 101400, China

^c School of Nanoscience and Technology, University of Chinese Academy of Sciences, Beijing 100049, China

^d Hunan Key Laboratory for Super Microstructure and Ultrafast Process, School of Physics and Electronics, Central South University, Changsha, Hunan 410083, China

^e School of Chemistry and Chemical Engineering, Hubei Polytechnic University, Huangshi 435003, China

^f School of Materials Science and Engineering, Georgia Institute of Technology, Atlanta, GA 30332-0245, United States

ARTICLE INFO

Keywords:

Mechanologic

Interactive

Triboelectric nanogenerator

Kirigami

Bistability

Digital logic

ABSTRACT

Mechanical logic and computation embedded in deployable structures are complementary to conventional digital logic schemes for autonomous sense, decision, and response in artificial intelligence and bio-robots. It is highly desired that responsive and adaptive structures can readily interact with external stimuli to implement mechanologic (e.g., writing, erasing, and rewriting mechanical bit) in an energy-efficient way. Here, we demonstrate kirigami interactive triboelectric mechanologic composed of a deployable kirigami geometry triggered by triboelectric signal for the first time, aiming at developing interactive and programmable mechanical computation. The interactive triboelectric mechanologic is inspired by human somatic reflex arc system to emulate the continual sensation–decision–response loop, which includes a self-powered triboelectric nanogenerator (TENG) mechanoreceptor, a signal transmission/processing module, and an elaborately designed kirigami geometry with bistable resistive states to represent mechanologic. When the mechanoreceptor is imposed to mechanical stimuli, the induced triboelectric signals activate the bistable state conversion in the kirigami geometry and endow it with adaptive capacity to output binary mechanical bits. We successfully demonstrate the application of interactive triboelectric mechanologic as a mechanical flip-flop, register, and asynchronous binary counter. This work provides a new route to self-activation mechanologic computation relying on the extended application of TENG for self-driven sensing and actuation.

1. Introduction

Intelligent robots are expected to interact with the ambient environment more quickly and precisely through an autonomous and adaptive self-control scheme. This requires unconventional mechanical logic units with programmable computation ability to be embedded into soft robots and implement in-memory sensing and computing to complement with conventional electronic logic units [1–4]. The essential point for embedded mechanologic units is to emulate the digital logic

language/configurations and conduct binary Boolean operations. Mechanical structures with reversible bistability are the primary option, which promises a basic mechanical bit for mechanical information memory and processing. To realize a complete mechanologic and computation system, relevant mechanical counterparts (e.g., interactive interface and logic gates) are also necessary to implement operation, transmission, and interaction on the stored mechanical information. Therefore, an energy-efficient way is critical for the mechanical counterparts to fulfill mechanologic conversion and complicated information

* Prof Zhong Lin Wang, an author on this paper, is the Editor-in-Chief of Nano Energy, but he had no involvement in the peer review process used to assess this work submitted to Nano Energy. This paper was assessed, and the corresponding peer review managed by Professor Chenguo Hu, also an Associate Editor in Nano Energy

* Corresponding author.

** Corresponding author at: Beijing Institute of Nanoenergy and Nanosystems, Chinese Academy of Sciences, Beijing 101400, China

E-mail addresses: xxyie@hbpu.edu.cn (X. Xie), zhong.wang@mse.gatech.edu (Z.L. Wang), sunqjun@binn.cas.cn (Q. Sun).

¹ These authors contributed equally to this work.

processing. For instance, relevant strategies include mechanical [5,6] and pneumatic actuators [1,2,7], shape memory polymer [8–11], and alloys that change shape in response to light, heat, magnetic, etc [12]. However, until now, the strategies for sophisticated interaction in a more energy-efficient way paired with a facile and economic mechanologic component on a common platform are still under seeking to extend broader and more practical applications.

Triboelectric nanogenerator (TENG), originated from Maxwell's displacement current [13], has offered an efficient way to micro/nano energy [14–16], self-powered sensing [17,18], high voltage source, blue energy [19,20], and even spectroscopy [21,22]. It operates on an effective energy budget that can harvest mechanical energy from the surrounding environment [23], supplying an ecosystem of self-powered sensors to interface with mechanical inputs [24–29]. The induced triboelectric potential can be readily utilized for interactive interface [17,30,31], driving transistors [21,22,32–42] and versatile sophisticated sensors [43–48]. Recently emerging contact-electrification activated afferents and mechano-tribotronic neuromorphic devices [21,22,41] have also delivered new possibilities toward integration of spatio-temporal information and neuromorphic computation, which is also an energy-efficient way to realizing interactive mechanical logic and computation. For the mechanologic component, kirigami is of particular interest due to its durable, low-cost, and lightweight material advantages [49–51]. It is also featured with huge design and operation space due to the facile and sophisticated deployable capacity and tunability [8, 52,53]. Furthermore, the concept of folding can be introduced into kirigami by using micromotors beyond the kirigami creases, which can be achieved through shape design and deformation through a self-driven manner. For bistable kirigami geometry, the momentary locking shape is the key to solving bistability of kirigami geometry [54]. Thus, it is required to develop how to temporally and spatially control shape formation and successfully implement a sensing mechanism that enables self-folding and instantaneous shape locking. Significantly, the diversified structure of mechanical components coupled with applicable and facile trigger methods will advance the wide application of mechanologic devices.

Here, we propose a kirigami interactive triboelectric mechanologic, which is composed of a deployable kirigami geometry triggered by triboelectric signal aiming at developing interactive and programmable mechanical computation. The interactive triboelectric mechanologic is inspired by human somatic reflex arc system to emulate the continual sensation–decision–response loop, which includes a self-activation TENG component (i.e., self-powered mechanoreceptor), a signal transmission/processing module, and an elaborately designed kirigami geometry with the bistable resistive state to represent mechanologic (i.e., a mechanical bit in the resistive state [0] and [1]). The kirigami geometry can be designed in stereo structure (rectangular/triangular pyramid, triangular prism, or other unfoldable shapes), which can be readily unfolded/folded along the bottom edges assisted with micromotors. An inner-mounted photoresistor is utilized to reflect two distinguished bistable resistive states when the photoresistor is exposed or unexposed to light under the unfolded or folded shape of the kirigami. When the TENG mechanoreceptor is imposed with mechanical action, the induced triboelectric signals activate the bistable state conversion based on the kirigami geometry and endow it with adaptive capacity to output binary mechanical bits relying on the recognition of external stimuli, i.e., interactive triboelectric mechanologic. We successfully demonstrate the application of the interactive triboelectric mechanologic as a mechanical flip-flop. Based on one mechanical bit in a single kirigami geometry, multibit Boolean operations and mechanical registers are also available by combining demanded numbers of the designed kirigami structure. As a proof of concept, four mechanical flip-flops are used to develop a mechanical behavior-derived asynchronous binary counter. The proposed kirigami triboelectric interactive framework demonstrates an energy-efficient way to programmable mechanologic and computation, offering a new idea for the extended application of TENG for self-driven

sensing in mechanical logic units.

2. Results and discussion

Mechanologic utilizes mechanical bits to store external mechanical information and implement the operation of mechanologic gates via specific signal transmission mechanisms (Fig. 1a). Generally, the mechanologic requires an interactive interface to communicate with external mechanical input, which is supplementary and compatible with conventional electronic controls by emulating the basic language and constitution of digital logic. Here, a deployable kirigami geometry harnessed with micromotor and photoresistor is designed as the basic mechanologic prototype as shown in Fig. 1b. The kirigami is designed in rectangular pyramid stereo structure (or triangular pyramid/prism), which can be readily unfolded/folded along the bottom edges assisted with micromotors. To endow the kirigami with bistable states, a photoresistor is mounted to the inner bottom facet. Thus, the bistable states can be represented in two distinguished resistive states ([0] or [1] state, bottom panel in Fig. 1b) when the photoresistor is exposed or unexposed to light under the unfolded or folded shape of the kirigami structure (determined by the angle between side face and bottom face, Fig. S1). Notably, stable numerical control micromotors paired with precise kirigami-geometry tailoring are critical to ensure distinguished bistability for subsequent mechanologic computation. As a basic mechanical bit that can switch between [0] and [1] states, the designed kirigami is also ready to be combined with multiple geometries to reconfigure multi-cell stereo structures with multibit capacity (this will be discussed later).

The interactive dynamic mechanologic is inspired by the continual sensation–decision–response ability of the human somatic reflex arc, which mainly involves three coordinated neurons: sensory neuron, relay neuron, and motor neuron (Fig. 1c). When an external stimulus affects the receptor (cell or organ that converts the stimulus into an electrical impulse), the sensory neuron carries impulse from the receptor to the central nervous system (CNS); then connector/relay neuron transmits the impulse slowly across the spinal cord; and finally motor neuron sends the impulse signal to the effector (either a muscle or a gland) to deliver the response. Analogously, the interactive dynamic mechanologic includes a self-powered mechanoreceptor, a signal processing module, and the designed kirigami geometry with mechanical computation capacity. Energy-efficient TENG is preferred as the self-activation sensor to constitute the ecosystem of mechanoreceptor, which is ready to utilize the harvested mechanical energy from surroundings to trigger the deployable kirigami. For the somatic reflex arc, the biological effector does not show any response until the action potential reaches a certain level. Similarly, a threshold should be set as a trigger voltage for the microcontroller to activate the kirigami structure for the implementation of mechanologic and computation (Fig. 1d). Thus, the triboelectric potential caused by mechanical action can be processed and trigger the deformation of the kirigami geometry to realize the logic conversion, i.e., interactive triboelectric mechanologic.

Single-electrode mode TENG (S-TENG, contact area is $7 \times 5 \text{ cm}^2$) composed of a silver electrode coated by polytetrafluoroethylene film (PTFE/Ag) is utilized as the interactive medium according to the facile structure and effective trigger efficiency (Fig. 2a and Fig. S2a). The operation principle of the as-designed S-TENG is schematically depicted in Fig. 2b. When the finger fully contacts with the PTFE friction layer (Fig. 2b(i)), opposite electrostatic charges are induced at the interface between PTFE and finger (there are electrons on the PTFE film and equivalent positive charges on the finger skin to maintain electrostatic equilibrium). When the finger is separated from the PTFE film (Fig. 2b(ii)), the electrostatic balance is broken and electrons will flow from the Ag electrode to the ground, leading to a positive voltage output. With the further separation between finger and S-TENG (Fig. 2b(iii)), the voltage output will reach the maximum value to conduct the effective trigger for mechanologic conversion. When the finger approaches PTFE film until

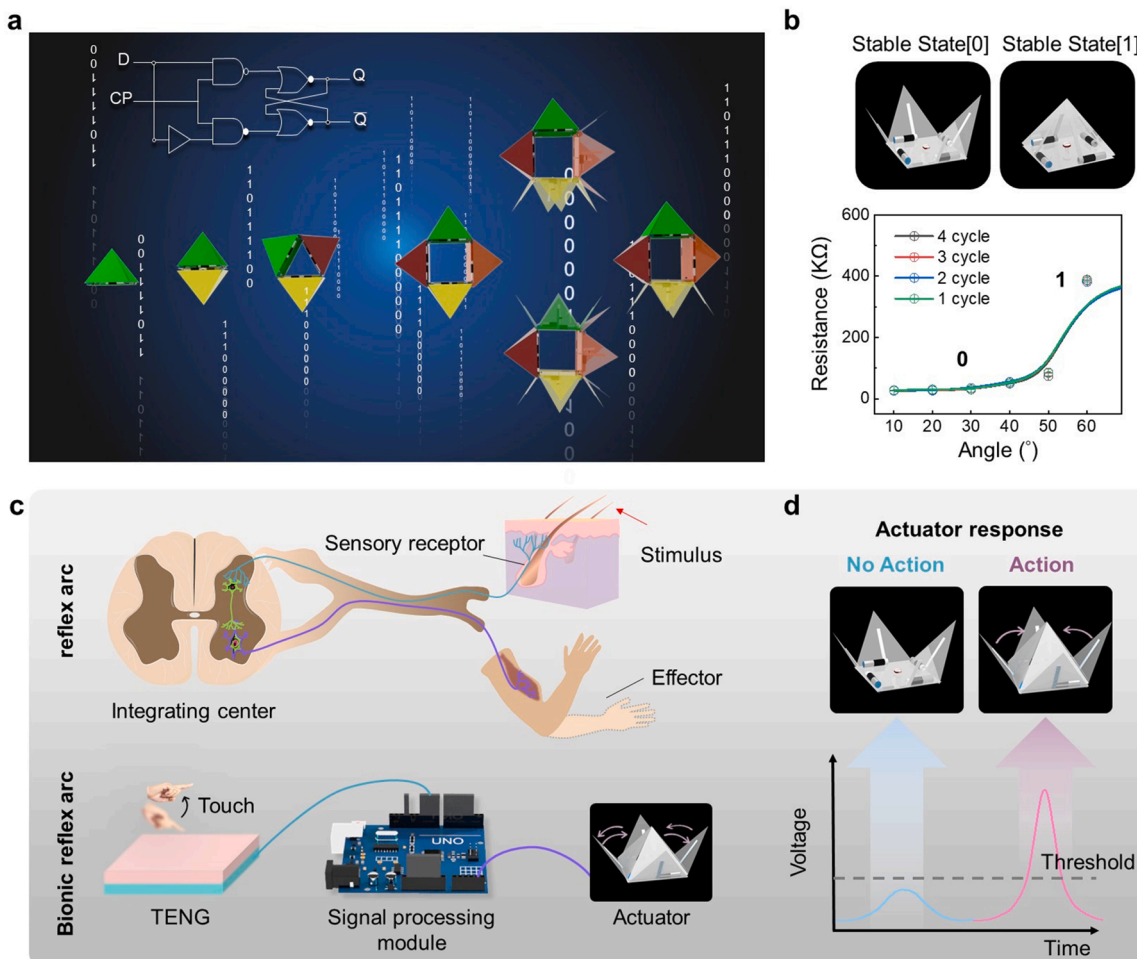


Fig. 1. The concept and state definition of mechanologic components for memory and calculation and bionic somatic nervous system. (a) The concept of the paper geometry mechanologic for information memory and calculation. (b) The [1] and [0] states of the unit; the resistance change between the two states is indicated. (c) The trigger mechanism of the bionic somatic nerve reflex. The somatic reflex arc consists of three main parts: sensory receptor (skin), integrating center (spinal cord), and effector (muscles). Correspondingly, our artificial electronic somatic reflex arc is composed of three devices as the counterparts: a TENG, a signal processing module (Arduino), and a designed paper geometry. (d) An actuator diagram that mimics the threshold-dependent response in a biological system. In our artificial reflex arc system, only when the voltage generated by TENG is higher than the threshold, the action of the actuator can be triggered.

they are in full contact with each other, the electrons will flow back from the ground to the Ag electrode to recover the initial electrostatic equilibrium (Fig. 2b(iv)). To evidence the working mechanism of the S-TENG interactive medium, finite element simulation is employed to verify the dynamic triboelectric potential distribution between a finger and PTFE film by using COMSOL. The simulated results indicate that the triboelectric potential difference between finger and PTFE film approaches 3.9 V with the separation distance increased from 0 to 30 mm, as shown in Fig. 2c.

Detailed electrical characterizations have also been carried out to investigate the output performance of the as-designed S-TENG mechanoreceptor. As shown in Fig. 2d, the open-circuit voltage (V_{OC}) increases from 0 to ~3.9 V upon contact-separation distance at 30 mm. Corresponding short-circuit current (I_{SC}) and transferred charge (Q_{SC}) are also recorded with maximum values at 18 nA and 1.5 nC, respectively (Fig. S2b-c). To achieve the effective implementation of mechanologic conversion (threshold is set to be > 2 V), the trigger voltage is also evaluated under several specific contact-separation distances (from 0 to 50 mm) aside from the simultaneously monitored pressures (ranging from 10.2 to 52.6 kPa, Fig. 2e). When the contact-separation distance is over 30 mm with monitored pressure to be over 17 kPa, the induced triboelectric voltage will be larger than 2 V and effectively trigger the unfolding process of the kirigami structure to implement logic

conversion. The responding time is monitored to be ~0.3 s (Fig. S2d). Furthermore, the stability of the TENG mechanoreceptor is characterized by monitoring the real-time V_{OC} of S-TENG for ~3000 s, which is essential for precisely triggering the mechanologic via triboelectricity. The V_{OC} can maintain a very stable output at 3.9 V with almost no fluctuations upon contact-separation at 30 mm (Fig. 2f). The above results all qualify the integrated S-TENG as an effective mechanoreceptor for mechanologic operation. For the signal processing module, we adopt a micro control unit (MCU, Arduino UNO) to synchronously detect the triboelectric voltage and convert the analog signal into H/L digital signal for implementing subsequent mechanologic (Fig. 2g). Effective paired touch actions (induce triboelectric voltage > 2 V) are demonstrated to trigger the unfolded and folded process of the kirigami with mechanologic (Fig. 2h and Movie S1), represented by two distinguishable and preservable resistive states.

Supplementary material related to this article can be found online at doi:10.1016/j.nanoen.2022.107345.

The interactive triboelectric mechanologic capture external mechanical stimuli, convert them into triboelectric signals, and trigger the reversible resistive logic states based on the designed kirigami structure. This process is consistent with the basic operation rule of a bistable flip-flop, which can be considered as a mechanical counterpart of this digital logic circuit. Fig. 3a shows the circuit configuration and working

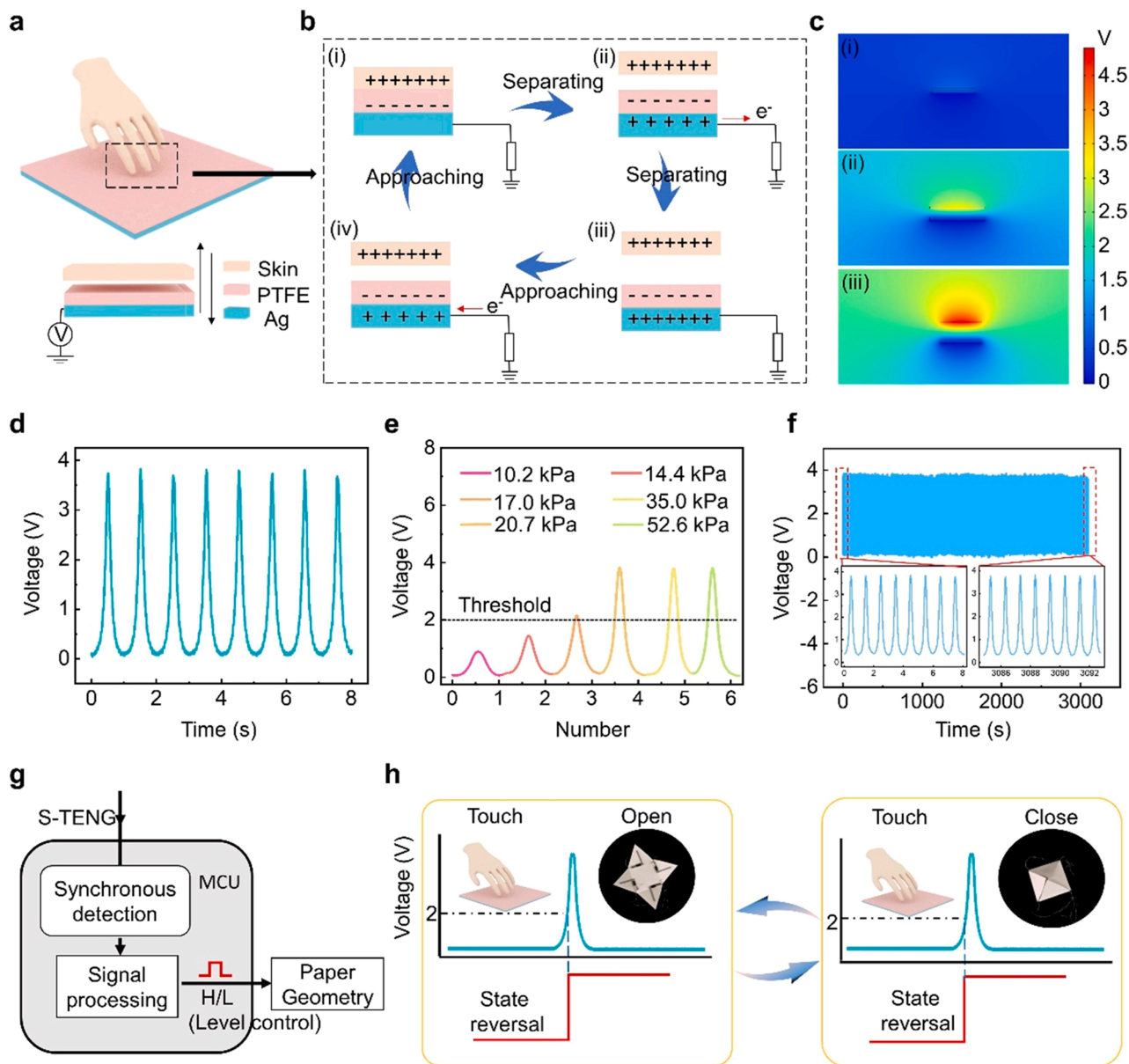


Fig. 2. Working principles and electrical output performance of the single-mode TENG. (a) Schematic illustration of hand touching on TENG. (b) Schematic diagram of working principles of the single-electrode mode TENG. (c) The COMSOL simulation results of the induced triboelectric potential. (d) V_{OC} of TENG in single-electrode mode. (e) The static voltage response of the TENG under different pressures. (f) The real-time voltage output of the S-TENG monitored for 3300 s (g) S-TENG is used for information interaction and paper geometry control. (h) Effective paired touch actions (induced triboelectric voltage > 2 V) are demonstrated to trigger the unfolded and folded process of the paper geometry.

principle of the bistable mechanical flip-flops. The mechanical flip-flop is characterized to have two stable states, which can be converted from one stable state to the other stable state after triggering by external mechanical action. Different from conventional digital logic circuits, input for the mechanical flip-flop is the triboelectric signal originating from the contact-electrification process when the TENG mechanoreceptor is imposed to external control/stimulus. The input triboelectric signal is captured and processed to activate the deformation of kirigami geometry and digitize the resultant mechanical states (via resistance) as output [1] (closed state) or [0] (opened state) (Fig. 3b). The process successfully implements the conversion from mechanical analog input signals to digital output signals through the interactive mechanologic. It can be written, erased, and rewritten between distinguished [1] and [0] resistive states, relying on the inner-mounted photoresistor under the closed or opened state of the kirigami geometry. The corresponding state

transition table of the mechanical flip-flop is illustrated in Fig. 3c. Thereinto, Q_n indicates the nominally previous state of the kirigami structure (open state is [0], closed state is [1]); D represents the mechanical stimuli/order applied to the mechanoreceptor (effective trigger = [1], ineffective trigger = [0]); Q_{n+1} indicates the subsequent state of the kirigami structure responding to the imposed external stimuli. The external stimuli input can readily trigger and store the bistable states in the mechanical flip-flop as shown in Movie S1.

Fig. 3d further shows the graphic symbol diagram of the mechanical flip-flop logic circuit, which flips at the rising of the clock pulse (CP) and synchronizes the TENG input data at the D-terminal with the clock to trigger the reversible states at the Q-terminal. The mechanical flip-flop can output corresponding mechanologic for given input stimuli (converted into triboelectric pulse signal) on the rising edge of the clock pulse and hold the state until it is imposed to a second triboelectric pulse

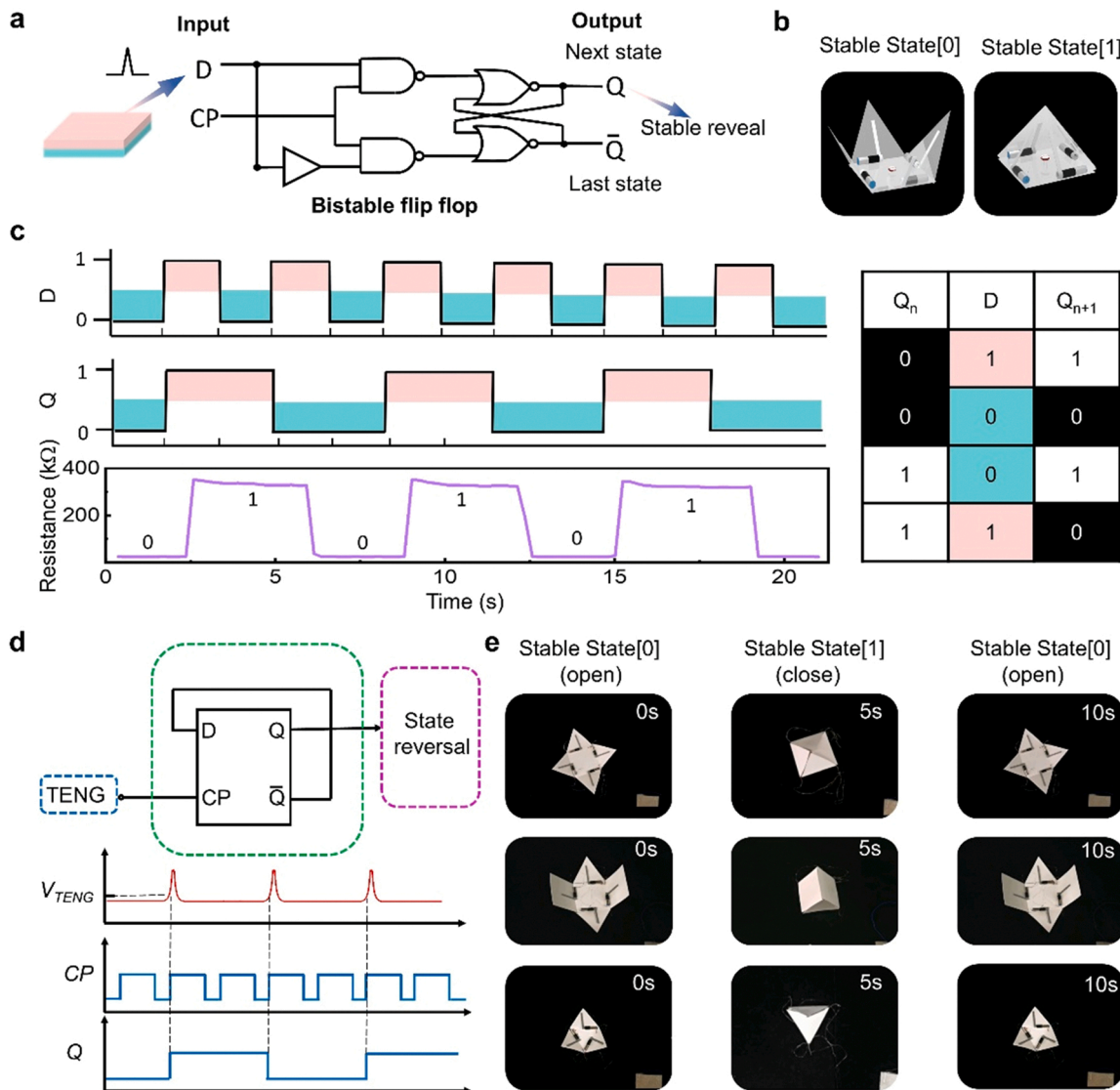


Fig. 3. Mechanologic unit as a flip-flop. (a) Schematics of the circuit configuration and working principle of the bistable mechanical flip-flops, which has inputs D (incoming data) and CP (clock) and output Q (stored data). D indicates the input of the TENG signal, Q is the state of the paper geometry (opening or closing). (b) A paper geometry writes, erases, and rewrites itself in response to time-varying stimuli and its state transition table. The resistance changes indicate the equilibrium configuration of the 1 and 0 states. (c) Corresponding truth table of the mechanical flip-flop. (d) The graphic symbol diagram of the mechanical flip-flop logic circuit and working waveform. (e) Kirigami mechanologic conversion for three different designs including quadrangular pyramids, triangles, and triangular prisms.

signal with next rising edge (bottom panel in Fig. 3d). Notably, kirigami geometry can also be readily designed into different heterostructures, e.g., rectangular/triangular pyramid, triangular prism, or other unfoldable shapes (Fig. 3e). All these kirigami geometries can be selected to implement relevant mechanologic on demands (Movie S1 to S3), which provides more possibilities to integrate with soft electronic components.

Supplementary material related to this article can be found online at doi:10.1016/j.nanoen.2022.107345.

Bistable flip-flops are building blocks for digital registers, synchronous binary counters, and sequential integrated circuits. For our mechanical flip-flop, it can be considered as a basic mechanical bit that can switch between [1] and [0] states. Multiple mechanical flip-flops are also ready to be combined into multi-cell stereo structures to realize reconfigured multibit capacity for register function. Each mechanologic unit can be individually controlled by one TENG to avoid interfering with other adjacent mechanologic units arranged in a distributed manner. Fig. 4a shows the graphic symbol diagram and working principle of the two-bit mechanical register which is composed of two connected mechanical flip-flops. The mechanical inputs can be applied to

Terminal-D₀ (or D₁) through mechanoreceptor TENG0 (or TENG1) sequentially or simultaneously. Terminal-Q₀ and Q₁ (denoting corresponding mechanologic output) can respond to the external stimuli with two mechanologic states based on the designed kirigami geometry in low or high resistive level (via the resistance change of the inner-mounted photoresistor). The configuration of the kirigami geometry based two-bit mechanical register in regular octahedron profile is represented in Fig. 4b, including two combined rectangular-pyramid-shaped kirigami geometries. The global logic states can be defined by a binary code [ij], where [i] and [j] denote the mechanologic state of the right and left units, respectively. For example, global state [01] indicates left kirigami in opened state accompanied with right kirigami in a closed state. When two peripheral TENG mechanoreceptors are imposed with mechanical touches as input orders, the induced triboelectric signal will be processed to follow the edge of the clock pulse (CP) and trigger relevant kirigami geometry to implement the reversible shape changes (Figs. 4b and S3). Accordingly, the global mechanologic state can be switched among four stable states, i.e., [00], [01], [11], and [10] states (the [10] marked in red frame is the fourth

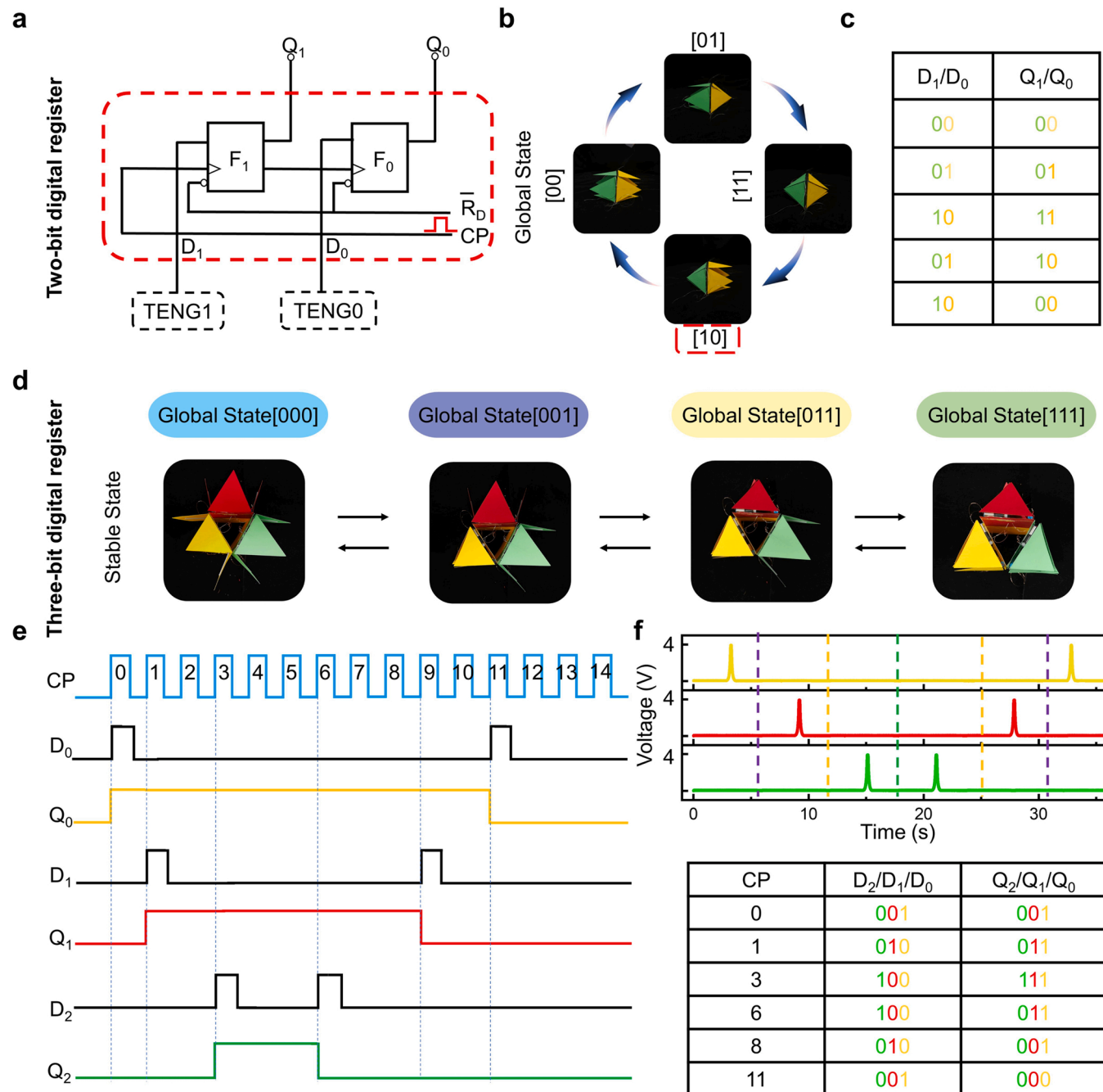


Fig. 4. Multi-bit binary mechanologic digital register. (a) The circuit structure of the two-bit digital register. (b) The configuration of the kirigami geometry based two-bit mechanical register. (c) Truth table of two-bit mechanical register. (d) Triboelectric potential actuation of multi-kirigami geometry leading to cyclic switch of states [000], [001], [011], and [111]. (e) Working waveform of three-bit mechanologic digital register. (f) The truth table of three-bit mechanologic digital register. The TENG trigger signal is corresponding to $D_2D_1D_0$.

stable state). The dynamic mechanologic conversion of the mechanical register in real-time is recorded as shown in Movie S3. The corresponding truth table of logic conversion in the two-bit mechanical register is shown in Fig. 4c. Starting from the mechanologic state [00] (two open-state kirigami geometries), we apply mechanical stimuli to TENG0 with TENG1 floating (input at Terminal D_1/D_0 is [01]), The induced triboelectric pulse signal in TENG0 will match the edge of the clock pulse and trigger the yellow kirigami geometry to be closed (mechanologic [1] state), while the floating TENG1 without imposed stimuli delivers no triggering order for the green geometry to maintain its initial open shape (mechanologic [0] state). Therefore, the output at Terminal- Q_1/Q_0 indicates a global mechanologic state of [01]. Sequentially,

when mechanical stimuli are only applied to TENG1 (input at D_1/D_0 is [10]), the green kirigami will be triggered to be closed with the output global mechanologic state changing to [11] (two closed-state kirigami). The following mechanical D_1/D_0 input [10] and [01] will lead to the Q_1/Q_0 mechanologic output at [01] and [00], respectively (following the truth table in Fig. 4c). This prototype of a two-bit mechanical register realizes the parallelism of arbitrary mechanical action input and the resultant fast response of mechanologic outputs at stable states, providing an efficient route to sensing, memory, and computation of mechanical information.

Based on the distributed activations of two combinational logic units for the two-bit mechanical register, we further explore assembling more

mechanologic units to enhance the programmability. Fig. 4d shows potential global states by combining three mechanological kirigami units in a triangle profile as a three-bit mechanical register. Three kirigami units are actuated by three individual TENG mechanoreceptors (i.e., three mechanical flip-flops). Corresponding symbolic diagram of the combined mechanical flip-flops is shown in Fig. S3b. Upon sequential stimuli imposed to TENG2, TENG1, and TENG0 as $D_2/D_1/D_0$ inputs of the mechanical flip-flops, the three mechanological kirigami units can be triggered to implement the shape conversion between closed and opened states accordingly (Movie S5), denoting global mechanologic states from [000] to [111] (represented by distinguished resistive states,

Fig. S3c). The actuation process via distributed TENG mechanoreceptors allows us to achieve sophisticated and selective three-bit mechanologic states. The induced triboelectric pulse signals paired with edges of clock pulses promise the precise triggering of the mechanological kirigami geometries (Fig. 4e and f). The mechanologic conversion at the sixth clock pulse is selected to be elaborated as an example. At clock pulse-6 with previous output logic state $Q_2/Q_1/Q_0$ in [111] (all close-state in three kirigami structures), when we only apply mechanical stimuli to TENG2 (the input at Terminal- $D_2/D_1/D_0$ is [100]), the green geometry is triggered to open, representing the global state at output Terminal- $Q_2/Q_1/Q_0$ is [011]. A complete truth table of the three-bit mechanical

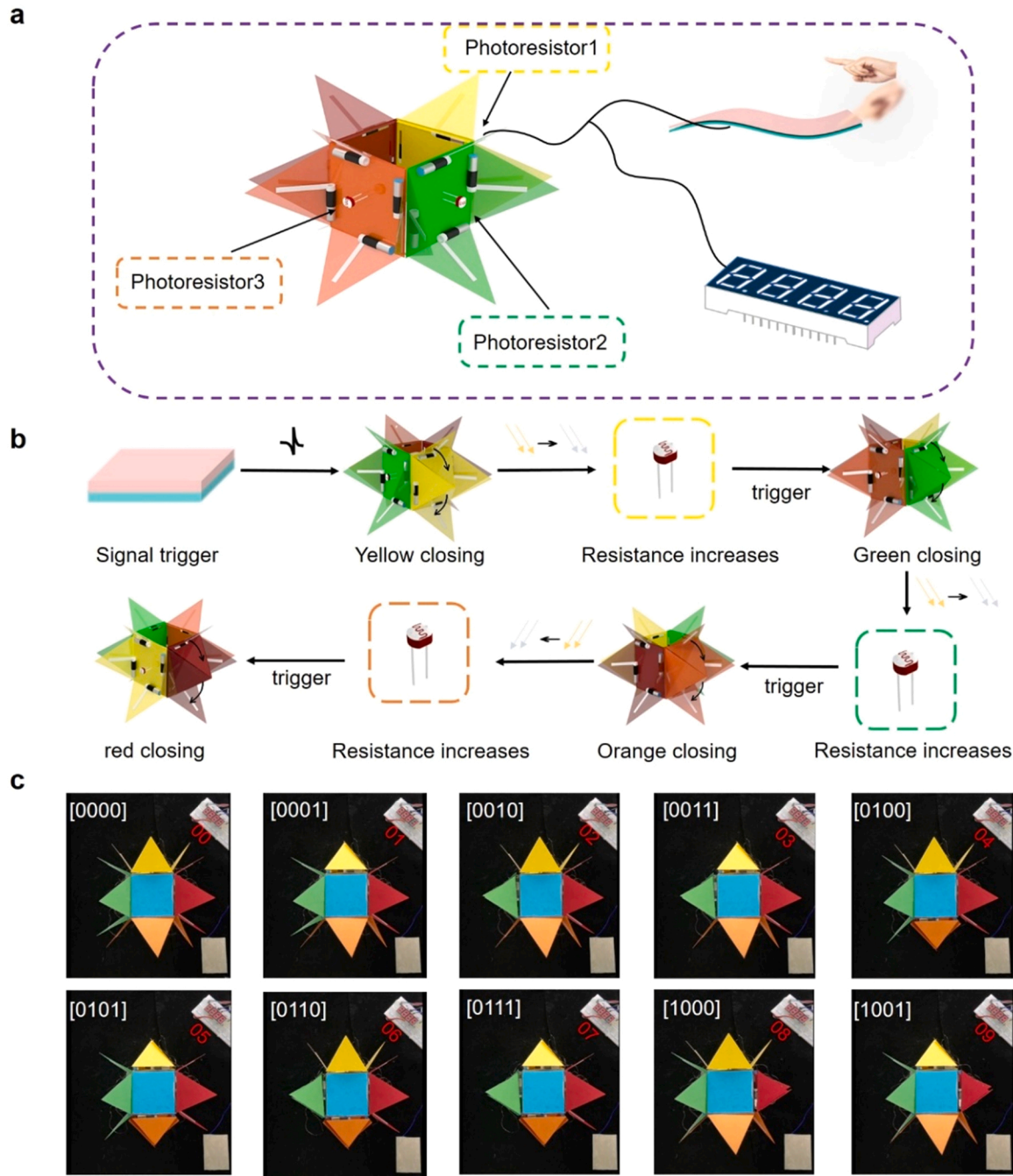


Fig. 5. An asynchronous four-bit binary counter consisting of four kirigami geometries for digital computing. (a) Schematic illustration diagram of a four-bit binary counter. (b) A simplified trigger mechanism diagram. Starting from the opened state, when TENG is triggered, the yellow FF₀ changes to the closed state [0], the resistance of the photoresistor1 increases which will trigger green unit cell; when the green FF₁ changes to the closed state [1], the resistance of the photoresistor2 increases which will trigger orange FF₂; when the orange FF₂ changes to the closed state [1], the resistance of the photoresistor3 increases which will trigger red unit cell. (c) Demonstration diagram of the whole counting process of an asynchronous four-bit binary counter.

register is shown in Fig. 4 f, indicating multiple global logic states are available to be triggered and stored in a reversible fashion. Furthermore, the TENG mechanoreceptors can be triggered simultaneously (or containing different temporal information), which promises potential sequential mechanologic applications.

Supplementary material related to this article can be found online at doi:10.1016/j.nanoen.2022.107345.

The designed kirigami units have been demonstrated for multibit mechanical registers, which integrate actuating, sensing, and potential memory capabilities to act as a basic logic module or integrated memory device. The electromechanical coupling between geometry units allows transmission of mechanical information and enables the implementation of mechanical logic gates that can be connected/combined to form reprogrammable mechanologic circuits. Besides, the bistable characteristics of mechanical output show its potential in representing binary systems hybrid with digital calculations, promising versatility beyond only structural reversibility for our interactive mechanologic system. Based on the demonstrated function of the digital register, the bistable mechanical flip-flops are also used for an asynchronous binary counter. As shown in Fig. 5a, the concept of the four-bit binary counter is illustrated, which is composed of three parts: TENG mechanoreceptor, four mechanological kirigami geometries (with inner-mounted photoresistors), and a digital display tube. Fig. 5b shows the asynchronous counting and sensing process based on the combined mechanical flip-flops. Four mechanological kirigami structures in open states are preset as the first stage. When the trigger TENG is activated by external stimuli (input logic is [1]), the yellow mechanological kirigami geometry will be closed (i.e., the output logic of the first mechanical flip-flops (FF₀) is [1]); At this stage, the resistance of photoresistor1 increases and the electrical signal is transmitted to trigger the green mechanological kirigami to be closed (output logic of the second FF₁ is [1]; This process leads to the resistance of photoresistor2 increases, delivering an induced electrical signal to trigger the orange mechanological kirigami geometry to be closed (output logic of the third FF₂ is [1]). Similarly, the third photoresistor3 shows an increased resistance, which triggers the final red mechanological kirigami geometry to be closed (output logic of the forth FF₃ is [1]). To realize the above asynchronous four-bit counting process, a specific electrical circuit diagram is designed as shown in Fig. S4. The TENG mechanoreceptor is connected with MCU terminal A0, and photoresistors are connected with terminal A1-A3, respectively. Both the TENG sensing signals and consequent resistance change of the photoresistors are the critical trigger signals to realize the entire mechanical counting process.

Corresponding symbolic circuit diagram of the four-bit mechanical binary counter is depicted in Fig. S5. TENG trigger signal is input to Terminal-D of the first flip-flop (FF₀), where each pulse input will lead to the state of FF₀ change once. The output Terminal-Q of the low-bit flip-flop is connected to the input Terminal-D of the next high-bit flip-flop. Whenever the state of the low-bit flip-flop (FF) changes from [0] to [1], a resultant positive jump pulse (as an input) is delivered to the adjacent high-bit FF, which leads to one flip of the high-bit FF (this is one binary addition counting process). To realize the consecutive function of addition counting, the photoresistor mounted in the kirigami structure with distinguished resistance change is critical to implement the “carry” function of the binary counter. More detailed asynchronous counting process is explained in supporting information Fig. S5.

The photo images of the four-bit mechanologic binary counter and corresponding logic outputs are shown in Fig. 5c. At the initial state without any stimuli input (input logic is [0]), the overall mechanologic output is [0000] (i.e., four kirigami are in opened state). When the TENG mechanoreceptor is triggered for the first time (input logic is [1]), the mechanologic output of the yellow kirigami FF₀ will be changed to [1] (yellow kirigami in closed state), and the overall mechanologic state is [0001] with the digital tube displaying the counting number as 1. When the TENG mechanoreceptor is triggered for the second time, the green kirigami FF₁ will receive the previous mechanologic [1] (yellow

kirigami in closed state) as the input and output itself as the second mechanologic state [1] (i.e., green kirigami in closed state), and the overall mechanologic is [0010] with a counting number 2. Accordingly, when the TENG mechanoreceptor is consecutively triggered for 10 times, the resultant logic state can be changed from [0000] to [1001] (also representing the counting number from 0 to 9 via the digital display tube, Fig. 5c). The detailed real-time counting process can be observed in Movie S6. These results indicate the successful demonstration of mechanical asynchronous binary counter based on the kirigami triboelectric mechanologic.

Supplementary material related to this article can be found online at doi:10.1016/j.nanoen.2022.107345.

3. Conclusion

This work provides a way to fabricating interactive kirigami geometries with bistability in a controllable, predictable, and continuous manner, which demonstrates how the mechanical logic cells can be combined to generate mechanical counting and computing systems. First, a complete sensing system is capable to complete the bistable conversion of the mechanical unit. To make the sensing process in an energy-efficient fashion, we use the self-powered and low-frequency TENG output signals to trigger the sensation–decision–response process of the mechanical unit. This idea is inspired by the human somatic reflex arc: a certain stimulus threshold is required to trigger the effector to respond; only a voltage signal above the threshold can be activated to trigger the mechanical actuator. The actuator reflects in the form of a mechanical bistable flip, whose mechanical state can be readily maintained according to the sophisticated kirigami structure design. The logic unit also possesses memory function, which has two stable working states and can be converted from one stable working state to another stable working state under the trigger of an external signal (regarded as a mechanical flip-flop). On this basis, more mechanical units can be combined to expand their memory and calculation functions.

In digital circuits, flip-flops are elementary components of digital registers and counters, so this work also visualizes these functions through these mechanical logic units. We combine multiple mechanical flip-flops to trigger one-by-one, which can realize the functions of parallel input and output of digital registers. More meaningfully, we use the TENG signal and the resistance signal of the photoresistor embedded in the mechanical unit as the sensing/transmitting signal at the same time. The photoresistor has a “carry” function, and the visual calculation process of the asynchronous binary counter circuit is completed. To extend the TENG self-driven sensing applications to control mechanical logic unit, this work demonstrates the potential of self-driven mechanical logic unit as a logic component and sequential logic circuit. More promisingly, this approach can be extended to other materials and more digital logic circuits.

4. Experiments

4.1. Fabrication and characterization of the TENG

For the design of the TENG mechanoreceptor, commercial silver tape was selected as the outer electrode, and PTFE was chosen as the friction material (the area of S-TENG is $7 \times 5 \text{ cm}^2$). To characterize the output measurement of TENG mechanoreceptor, the contact-separation action was applied by a commercial linear mechanical motor. TENG output performances were measured by an electrometer (Keithley 6541 system). The surface charge density is $4.33 \times 10^{-7} \text{ C/m}^2$. A custom LabVIEW program was used to record the electrical output. A force detector (YMC 501F01, 8 mm diameter) was used to sense the applied force. The external force was also applied by the linear mechanical motor and monitored by an oscilloscope.

4.2. Fabrication of kirigami geometry unit

We manufacture each kirigami geometric unit by cutting the patterns with a laser-cutting machine and fixing the kirigami sheet on the motor and the shaft which is fixed on the motor. Actuation is provided by a motor fixed in parallel to the actuation axis (Miniature planetary gear motor, 6 mm diameter, 35 g.cm holding torque, DC 1.2–4.2 v). The axis is firstly designed by 3Dmax and converted into a pattern that can be recognized by the 3D printer with Flash-Print software, and then printed by the 3D printer.

4.3. Fabrication of four-digit binary counter

The four-digit binary counter is composed of three parts: TENG, four kirigami geometries, photoresistors, and digital display tubes. To construct the circuit, a photoresistor is attached inside the unit cell to realize the carry function of the counter: photoresistor1 is connected in series to the second mechanical flip-flop whose output is the mechanical state of the green cell; photoresistor2 is connected in series to the mechanical state of the output of the third mechanical flip-flop; The photoresistor3 is connected in series to the fourth mechanical flip-flop whose output is the mechanical state of the red cell. The digital tube is connected to the TENG input which would display the digital signal converted by mechanical deformation memory.

Declaration of Competing Interest

The authors declare that they have no known competing financial interests or personal relationships that could have appeared to influence the work reported in this paper.

Acknowledgment

This work is financially supported by the National Key Research and Development Program of China (2021YFB3200304), the National Natural Science Foundation of China (52073031), Beijing Nova Program (Z191100001119047, Z211100002121148), Fundamental Research Funds for the Central Universities (EOEG6801×2), and the “Hundred Talents Program” of the Chinese Academy of Science.

Appendix A. Supporting information

Supplementary data associated with this article can be found in the online version at [doi:10.1016/j.nanoen.2022.107345](https://doi.org/10.1016/j.nanoen.2022.107345).

References

- [1] D.J. Preston, P. Rothmund, H.J. Jiang, M.P. Nemitz, J. Rawson, Z. Suo, G. M. Whitesides, Digital logic for soft devices, *Proc. Natl. Acad. Sci.* 116 (16) (2019) 7750–7759.
- [2] L. Paez, G. Agarwal, J. Paik, Design and analysis of a soft pneumatic actuator with origami shell reinforcement, *Soft Robot.* 3 (3) (2016) 109–119.
- [3] T. Mei, Z. Meng, K. Zhao, C.Q. Chen, A mechanical metamaterial with reprogrammable logical functions, *Nat. Commun.* 12 (1) (2021) 7234.
- [4] P. Zhou, J. Lin, W. Zhang, Z. Luo, L. Chen, Pressure-perceptive actuators for tactile soft robots and visual logic devices, *Adv. Sci.* 9 (5) (2022), 2104270.
- [5] P. Bhowad, J. Kaufmann, S. Li, Peristaltic locomotion without digital controllers: Exploiting multi-stability in origami to coordinate robotic motion, *Extrem. Mech. Lett.* 32 (2019), 100552.
- [6] S. Kamrava, D. Mousanezhad, S.M. Felton, A. Vaziri, Programmable origami strings, *Adv. Mater. Tech.* 3 (3) (2018), 1700276.
- [7] A. Oyefusi, J. Chen, Reprogrammable chemical 3D shaping for origami, kirigami, and reconfigurable molding, *Angew. Chem. Int. Ed.* 56 (28) (2017) 8250–8253.
- [8] T. van Manen, S. Janbaz, M. Ganjian, A.A. Zadpoor, Kirigami-enabled soft-folding origami, *Mater. Today* 32 (2020) 59–67.
- [9] Y. Hu, A. Xu, J. Liu, L. Yang, L. Chang, M. Huang, W. Gu, G. Wu, P. Lu, W. Chen, Y. Wu, Multifunctional soft actuators based on anisotropic paper/polymer bilayer toward bioinspired applications, *Adv. Mater. Tech.* 4 (2019), 1800674.
- [10] B. Treml, A. Gillman, P. Buskohl, R. Vaia, Origami mechanologic, *Proc. Natl. Acad. Sci.* 115 (27) (2018) 6916–6921.
- [11] G.Z. Lum, Z. Ye, X. Dong, H. Marvi, O. Erin, W. Hu, M. Sitti, Shape-programmable magnetic soft matter, *Proc. Natl. Acad. Sci.* 113 (41) (2016) 6007–6015.
- [12] L.S. Novelino, Q. Ze, S. Wu, G.H. Paulino, R. Zhao, Untethered control of functional origami microrobots with distributed actuation, *Proc. Natl. Acad. Sci.* 117 (39) (2020) 24096–24101.
- [13] Z.L. Wang, On Maxwell's displacement current for energy and sensors: the origin of nanogenerators, *Mater. Today* 20 (2) (2017) 74–82.
- [14] G. Zhu, P. Bai, J. Chen, Z.L. Wang, Power-generating shoe insole based on triboelectric nanogenerators for self-powered consumer electronics, *Nano Energy* 2 (5) (2013) 688–692.
- [15] G. Li, S. Fu, C. Luo, P. Wang, Y. Du, Y. Tang, Z. Wang, W. He, W. Liu, H. Guo, J. Chen, C. Hu, *Nano Energy* 96 (2022), 107068.
- [16] J. Zhang, S. Hu, Z. Shi, Y. Wang, Y. Lei, J. Han, Y. Xiong, J. Sun, L. Zheng, Q. Sun, G. Yang, Z.L. Wang, Eco-friendly and recyclable all cellulose triboelectric nanogenerator and self-powered interactive interface, *Nano Energy* 89 (2021), 106354.
- [17] J. Huang, X. Yang, J. Yu, J. Han, C. Jia, M. Ding, J. Sun, X. Cao, Q. Sun, Z.L. Wang, A universal and arbitrary tactile interactive system based on self-powered optical communication, *Nano Energy* 69 (2020), 104419.
- [18] G. Li, G. Liu, W. He, L. Long, B. Li, Z. Wang, Q. Tang, W. Liu, C. Hu, *Nano Res.* 14 (2021) 4204.
- [19] Z.L. Wang, T. Jiang, L. Xu, Toward the blue energy dream by triboelectric nanogenerator networks, *Nano Energy* 39 (2017) 9–23.
- [20] Y. Zhang, Y. Li, R. Cheng, S. Shen, J. Yi, X. Peng, C. Ning, K. Dong, Z.L. Wang, Underwater Monitoring Networks Based on Cable-Structured Triboelectric Nanogenerators, *Research* (2022), 9809406.
- [21] J. Yu, X. Yang, G. Gao, Y. Xiong, Y. Wang, J. Han, Y. Chen, H. Zhang, Q. Sun, Z. L. Wang, Bioinspired mechano-photonic artificial synapse based on graphene/MoS² heterostructure, *Sci. Adv.* 7 (12) (2021) eabd9117.
- [22] J. Yu, G. Gao, J. Huang, X. Yang, J. Han, H. Zhang, Y. Chen, C. Zhao, Q. Sun, Z. L. Wang, Contact-electrification-activated artificial afferents at femtojoule energy, *Nat. Commun.* 12 (1) (2021) 1–10.
- [23] C. Wu, X. Wang, L. Lin, H. Guo, Z.L. Wang, Paper-based triboelectric nanogenerators made of stretchable interlocking kirigami patterns, *ACS Nano* 10 (4) (2016) 4652–4659.
- [24] Z. Zhou, L. Weng, T. Tat, A. Libanori, Z. Lin, L. Ge, J. Yang, J. Chen, Smart insole for robust wearable biomechanical energy harvesting in harsh environments, *ACS Nano* 14 (10) (2020) 14126–14133.
- [25] J. Han, C. Xu, J. Zhang, N. Xu, Y. Xiong, X. Cao, Y. Liang, L. Zheng, J. Sun, J. Zhai, Q. Sun, Z.L. Wang, Multifunctional coaxial energy fiber toward energy harvesting, storage, and utilization, *ACS Nano* 15 (1) (2021) 1597–1607.
- [26] W. Alquraishi, Y. Fu, W. Qiu, J. Wang, Y. Chen, L. Kong, J. Sun, Y. Gao, Hybrid optoelectronic synaptic functionality realized with ion gel-modulated In₂O₃ phototransistors, *Org. Electron.* 71 (2019) 72–78.
- [27] S. Qin, Q. Zhang, X. Yang, M. Liu, Q. Sun, Z.L. Wang, Hybrid piezo/triboelectric-driven self-charging electrochromic supercapacitor power package, *Adv. Energy Mater.* 8 (2018), 1800069.
- [28] Y. Yang, J. Han, J. Huang, J. Sun, Z.L. Wang, S. Seo, Q. Sun, Stretchable energy-harvesting tactile interactive interface with liquid-metal-nanoparticle-based electrodes, *Adv. Funct. Mater.* 30 (2020), 1909652.
- [29] J. Han, N. Xu, Y. Liang, M. Ding, J. Zhai, Q. Sun, Z.L. Wang, Paper-based triboelectric nanogenerators and their applications: a review, *Beilstein J. Nanotechnol.* 12 (2021) 151–171.
- [30] J. Huang, X. Yang, J. Yu, J. Han, C. Jia, M. Ding, J. Sun, X. Cao, Q. Sun, Z.L. Wang, A universal and arbitrary tactile interactive system based on self-powered optical communication, *Nano Energy* 69 (2020), 104419.
- [31] D.H. Ho, J. Han, J. Huang, Y.Y. Choi, S. Cheon, J. Sun, Y. Lei, G.S. Park, Z.L. Wang, Q. Sun, J.H. Cho, β -Phase-Preferential blow-spun fabrics for wearable triboelectric nanogenerators and textile interactive interface, *Nano Energy* 77 (2020), 105262.
- [32] J. Yan, Y. Chen, X. Wang, Y. Fu, J. Wang, J. Sun, G. Dai, S. Tao, Y. Gao, High-performance solar-blind SnO₂ nanowire photodetectors assembled using optical tweezers, *Nanoscale* 11 (5) (2019) 2162–2169.
- [33] C. Qian, L. Kong, J. Yang, Y. Gao, J. Sun, J. Multi-Gate Organic Neuron Transistors for Spatiotemporal Information Processing, *Appl. Phys. Lett.* 110 (2017), 083302.
- [34] H. Zhang, J. Yu, X. Yang, G. Gao, S. Qin, J. Sun, M. Ding, C. Jia, Q. Sun, Z.L. Wang, Ion gel capacitively coupled triboionic gating for multiparameter distance sensing, *ACS Nano* 14 (3) (2020) 3461–3468.
- [35] X. Yang, J. Yu, J. Zhao, Y. Chen, G. Gao, Y. Wang, Q. Sun, Z.L. Wang, Mechanoplastic triboionic floating-gate neuromorphic transistor, *Adv. Funct. Mater.* 30 (34) (2020), 2002506.
- [36] J. Sun, Y. Fu, Q. Wan, Organic synaptic devices for neuromorphic systems, *J. Phys. D: Appl. Phys.* 51 (31) (2018), 314004.
- [37] Y. Chen, G. Gao, J. Zhao, H. Zhang, J. Yu, X. Yang, Q. Zhang, W. Zhang, S. Xu, J. Sun, Y. Meng, Q. Sun, Piezotronic Graphene Artificial Sensory Synapse, *Adv. Funct. Mater.* 29 (41) (2019), 1900959.
- [38] S. Kim, Y.J. Choi, H.J. Woo, Q. Sun, S. Lee, M.S. Kang, Y.J. Song, Z.L. Wang, J. H. Cho, Piezotronic graphene barristor: Efficient and interactive modulation of Schottky barrier, *Nano Energy* 50 (2018) 598–605.
- [39] G. Gao, B. Wan, X. Liu, Q. Sun, X. Yang, L. Wang, C. Pan, Z.L. Wang, Tunable Tribotronic Dual-Gate Logic Devices Based on 2D MoS₂ and Black Phosphorus, *Adv. Mater.* 30 (13) (2018), 1705088.
- [40] X. Yang, J. Han, J. Yu, Y. Chen, H. Zhang, M. Ding, C. Jia, J. Sun, Q. Sun, Z. L. Wang, Versatile Triboiontronic Transistor via Proton Conductor, *ACS Nano* 14 (7) (2020) 8668–8677.
- [41] F. Tan, Y. Xiong, J. Yu, Y. Wang, Y. Li, Y. Wei, J. Sun, X. Xie, Q. Sun, Z.L. Wang, Triboelectric potential tuned dual-gate IGZO transistor for versatile sensory device, *Nano Energy* 90 (2021), 106617.

- [42] W. Liu, J. Sun, W. Qiu, Y. Chen, Y. Huang, J. Wang, J. Yang, Sub-60 mV per decade switching in ion-gel-gated In-Sn-O transistors with a nano-thick charge trapping layer, *Nanoscale* 11 (2019) 21740–21747.
- [43] W. Qiu, J. Sun, W. Liu, Y. Huang, Y. Chen, J. Yang, Y. Gao, Multi-gate-driven In-Ga-Zn-O memtransistors with a Sub-60 mV/decade subthreshold swing for neuromorphic and memlogic applications, *Org. Electron.* 84 (2020), 105810.
- [44] J. Yu, S. Qin, H. Zhang, Y. Wei, X. Zhu, Y. Yang, Q. Sun, Fiber-shaped triboiontronic electrochemical transistor, *Research* (2021), 9840918.
- [45] J. Wang, Y. Chen, K. L.-A, Y. Fu, Y. Gao, S, J, Deep-ultraviolet-triggered neuromorphic functions in In-Zn-O phototransistors, *Appl. Phys. Lett.* 113 (15) (2018), 151101.
- [46] Q. Sun, D.H. Kim, S.S. Park, N.Y. Lee, Y. Zhang, J.H. Lee, K. Cho, J.H. Cho, Transparent, low-power pressure sensor matrix based on coplanar-gate graphene transistors, *Adv. Mater.* 26 (27) (2014) 4735–4740.
- [47] Y. Huang, W. Qiu, W. Liu, C. Jin, J. Sun, J. Yang, Non-Volatile In-Ga-Zn-O transistors for neuromorphic computing, *Appl. Phys. A: Mater. Sci. Proc.* 27 (5) (2021) 1–10.
- [48] W. Alquraishi, J. Sun, W. Qiu, W. Liu, Y. Huang, C. Jin, Y. Gao, Mimicking optoelectronic synaptic functions in solution-processed In-Ga-Zn-O phototransistors, *Appl. Phys. A: Mater. Sci. Proc.* 126 (2020) 1–7.
- [49] B. An, S. Miyashita, A. Ong, M.T. Tolley, M.L. Demaine, E.D. Demaine, R.J. Wood, D. Rus, An end-to-end approach to self-folding origami structures, *IEEE Trans. Robot.* 34 (6) (2018) 1409–1424.
- [50] D. Rus, M.T. Tolley, Design, fabrication and control of origami robots, *Nat. Rev. Mater.* 3 (6) (2018) 101–112.
- [51] R. Ma, C. Wu, Z.L. Wang, V.V. Tsukruk, Pop-up conducting large-area biographene kirigami, *ACS Nano* 12 (10) (2018) 9714–9720.
- [52] L.C. Wang, W.L. Song, D. Fang, Twistable origami and kirigami: from structure-guided smartness to mechanical energy storage, *ACS Appl. Mater. Inter.* 11 (3) (2019) 3450–3458.
- [53] J.J. Park, P. Won, S.H. Ko, A review on hierarchical origami and kirigami structure for engineering applications, *Inter. J. Precis. Eng. Manufact. Tech.* 6 (1) (2019) 147–161.
- [54] Z. Meng, W. Chen, T. Mei, Y. Lai, Y. Li, C.Q. Chen, Bistability-based foldable origami mechanical logic gates, *Extrem. Mech. Lett.* 43 (2021), 101180.